ISSN 1070-3284, Russian Journal of Coordination Chemistry, 2013, Vol. 39, No. 8, pp. 620–627. © Pleiades Publishing, Ltd., 2013.

pH-Dependent Syntheses and Crystal Structures, Characterizations, and DFT Calculations of Complexes with 2,2'-Biimidazole and Terephthalic Acid Ligands[1]

L. N. Yang[a, b], C. H. Zhou[c], Y. X. Zhi[a], J. H. Hei[a], J. Li[a], and F. X. Zhang[a, *]

[a] *Key Laboratory of Synthetic and Natural Functional Molecule Chemistry of Ministry of Education, College of Chemistry & Materials Science, Northwest University, Xi'an, Shaanxi, 710069 P.R. China*

[b] *Department of Pharmacy, Xi'an Medical University, Shaanxi, 710021 P.R. China*

[c] *Institute for Chemical Physics & Department of Chemistry, Faculty of Science, Xi'an Jiaotong University, Xi'an, 710049 P.R. China*

**e-mail: zhangfx@nwu.edu.cn*

Received January 23, 2012

Abstract—The divalent transition metal complexes $[Zn(L)_2(H_2O)_2](Tere)$ (**I**), $[Cd(L)_2(H_2O)_2](Tere])$ (**II**) and $[Cd(L)_2(HTere)_2]$ (**III**) (L = 2,2'-biimidazole, Tere = terephthalate) have been synthesized under hydrothermal conditions and characterized by elemental analysis, IR spectrum, thermal analysis and single-crystal X-ray diffraction analysis. Complexes **II** and **III** have the same starting materials but possess different frameworks and are prepared from H_2Biim and H_2Tere under hydrothermal conditions with different pH values. The crystal structures show **I** and **II** have the same coordination circumstances and are coordinated by two H_2O molecules and two neutral bidentate 2,2'-biimidazole ligands. The terephthalate acts as the counter anion. In contrast, complex **III** contains protonated carboxylate groups coordinated to the metal centre to give neutral species. Furthermore, based on the optimized structures, molecular frontier orbitals, Mulliken charges and IR spetra of complex **I** and **III** are investigated by density functional theory. Calculated results show that the energy gap (ΔE_{L-H}) between HOMO and LUMO of complex **III** is bigger than that of **I**. It is revealed that complex **III** is more stable, and this calculated estimation corresponds with experimental analysis of TGA curves.

DOI: 10.1134/S1070328413080101

INTRODUCTION

Supramolecular assemblies have provided numerous materials with very attractive properties [1]. There is currently great interest in rational design of new structures with specific architectures in one, two and three dimensions. The rational design and controllable preparation of new structures, which is highly influenced by several factors, for instance, the coordination geometry of the central atom, the structural characteristics of the ligand molecule, the counter anion, the pH values of the reaction solutions, symmetry the solvent system, the reaction conditions and so on [2–6]. Thus, it is possible to synthesize polymeric frameworks with interesting topologies through the appropriate reaction conditions. The pH values of the reaction, as one of the external factor, is especially important in the assembly of supramolecular architectures. It not only affects the ligand coordination ability but also the metal-to-ligand ratio, and consequently, the resulting structures [7–13].

In this work, we chose the widely used organic ligands 2,2'-biimidazole (H_2Biim) and aromatic carboxylate (terephthalic acid) as an example to show the role of the pH values of the reaction in controlling the structure of the supramolecular architecture and report here hydrothermal synthesis, crystal structures, and thermal properties of $[Zn(L)_2(H_2O)_2](Tere)$ (**I**), $[Cd(L)_2(H_2O)_2](Tere)$ (**II**), and $[Cd(L)_2(HTere)_2]$ (**III**) (L = 2,2'-imidazole, Tere = terephthalate). Currently, density functional theory (DFT) is an important theoretical method for investigation of molecular geometrical and electronic structure. It meets with the requirements of being accurate, easy to use, and fast enough to allow the study of relatively large molecules of transition metal complexes [14, 15]. Therefore, geometrical structures, frontier orbitals energies, Mulliken charge distributions, and IR spetra of complexes **I** and **III** are calculated by B3LYP/LANL2DZ method in this work.

EXPERIMENTAL

Materials and methods. 2,2'-Biimidazole was prepared as described previously in the literature [1, 16]. The other reagents were of analytical grade from commercial sources and were used without any further

[1] The article is published in the original.

purification. Elemental analysis was performed by Vario EL-III instrument. Infrared spectrum was recorded on an Equinox55 spectrophotometer in the range of 4000–400 cm^{-1} using a powdered sample on a KBr pellet. Thermal analysis was performed on a Netzsch STA 449C instrument, with a heating rate of 10°C/min in nitrogen. DFT calculations were performed by using GAUSSIAN 03 program.

Synthesis of I. A mixture of $Zn(NO_3)_2 \cdot 6H_2O$ (0.0892 g, 0.3 mmol), H_2Biim (0.0402 g, 0.3 mmol), terephthalic acid (0.0498 g, 0.3 mmol), and deionized water (5 mL) was adjusted to pH 7–8 with aqueous KOH solution, further stirred for 30 min in air, and then transferred and sealed in a Teflon-lined stainless vessel (25 mL) and heated at 160°C for 6 days under autogenous pressure. Afterwards, the vessel was cooled to room temperature at a rate of 10°C h^{-1}. The sheet-like colourless crystals of complex **I** was obtained. The yield was 20%.

FT-IR (KBr; ν, cm^{-1}): 3127–2791 br., m, 1567 s, 1522 m, 1399 v.s, 1123 m, 992 m, 758 m, 689 m.

For $C_{20}H_{20}N_8O_6Zn$

anal. calcd., %:	C, 45.17;	H, 3.44;	N, 21.47.
Found, %:	C, 45.03;	H, 3.75;	N, 21.01.

Synthesis of II. Complex **II** was synthesized by an analogous procedure as **I**, except using of $CdCl_2 \cdot 2.5H_2O$ (0.0685 g, 0.3 mmol) instead of $Zn(NO_3)_2 \cdot 6H_2O$. The light yellow block crystals of complex **II** was obtained in pH 7–8 and heating at 160°C for 6 days. The yield was 50%.

FT-IR (KBr; ν, cm^{-1}): 3165–2742 br., m, 1566 s, 1524 m, 1386 v.s, 1125 m, 994 m, 767 m, 689 m.

For $C_{20}H_{20}N_8O_6Cd$

anal. calcd., %:	C, 41.38;	H, 3.45;	N, 19.31.
Found, %:	C, 40.89;	H, 3.13;	N, 19.31.

Synthesis of III. Complex **III** was synthesized analogously **II**, except the pH values (5–6) of the reaction. The heating at 160°C for 6 days gives the light purple block crystals of complex **III**. The yield was 45%.

FT-IR (KBr; ν, cm^{-1}): 3126–2542 br., m, 1692 s, 1588 s, 1555 m, 1429 m, 1371 v.s, 1124 m, 992 m, 741 m, 690 m.

For $C_{28}H_{22}N_8O_8Cd$

anal. calcd., %:	C, 47.25;	H, 2.77;	N, 15.97.
Found, %:	C, 47.30;	H, 3.10;	N, 15.77.

X-ray diffraction analysis. Diffraction data for **I**, **III** were collected on a Bruker Smart APEX CCD diffractometer using the ω-scan technique. The structures were solved by direct methods and least-squares refinement was performed with the SHEXTL-97 program [17]. All non-hydrogen atoms were refined anisotropically and hydrogen atoms were place in calculated positions with respect to the isotropic displacement parameters. The crystallographic data for **I** and **III** are summarized in Table 1. Select bond distances and bond angles are given in Table 2. The hydrogen bonds are given in Table 3. Supplementary material has been deposited with the Cambridge Crystallographic Data Centre (nos. 603833 (**I**) and 603424 (**III**); deposit@ccdc.cam.ac.uk or http://www.ccdc.cam.ac.uk).

RESULTS AND DISCUSSION

Complexes **I**–**III** were prepared through hydrothermal reactions of the similar precursors. Only the pH values of the reaction was different by controlling amount of KOH, especially the complex **II** was formed from the same staring materials as complex **III** as shown in Scheme. Since the only difference in synthetic conditions among **II** and **III** is the pH value of the reactions, their structural differences ambiguously indicate that the assembly process is pH-dependent. the pH value of the reaction is, in fact, indicative of deprotonated extent of H_2Tere in the reaction. At pH 7–8, being highly deprotonated, the concentration ratio of Tere to HTere is high, and the complex with low ratio of HTere to Tere would be expected, and H_2O coordinated to Cd easily. At pH 5–6, the concentration ratio of HTere would be increased in comparison with the reaction of **II**. The coordinated water at the basal plane in **II** is replaced by HTere ligand, and the neutral species of **III** is formed. The synthesis of the complexes described here demonstrates that similar precursors can be used to obtain different structures by varying only the pH values of the reaction.

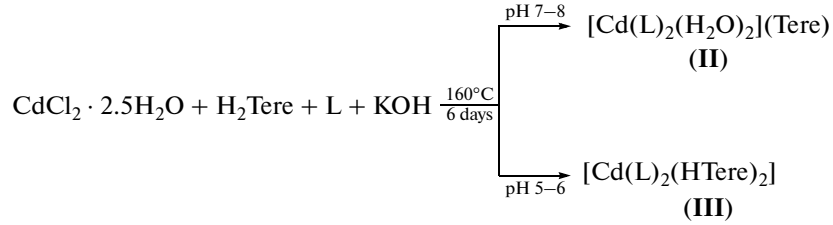

Scheme.

Table 1. Crystal data and structure refinement for complexes **I** and **III**

Parameter	Value	
	I	**III**
Formula weight	533.81	710.94
Crystal size, mm	0.41 × 0.16 × 0.05	0.42 × 0.38 × 0.20
T, K	298(2)	295(2)
Crystal system	Monoclinic	Monoclinic
Space group	$P2(1)/n$	$P2(1)/n$
a, Å	8.1911(10)	7.3824(4)
b, Å	10.8763(14)	13.3772(8)
c, Å	12.6257(16)	14.8040(8)
β, deg	94.560(2)	103.693(1)
V, Å^3	1121.2(2)	1420.4(1)
Z	2	2
ρ_{calcd}, g cm^{-3}	1.581	1.662
$F(000)$	548	716
θ Range, deg	2.47–25.10	2.8–27.7
Index ranges h, k, l	$-9 \le h \le 7, -11 \le k \le 12, -15 \le l \le 14$	$-9 \le h \le 7, -13 \le k \le 17, -18 \le l \le 19$
Absorption coefficient, mm^{-1}	1.151	0.835
GOOF (F^2)	1.069	1.11
Reflections collected/independent (R_{int})	6955/2753 (0.0243)	8385/3250 (0.030)
Reflections with ($I > 2\sigma(I)$)		
Final R indices ($I > 2\sigma(I)$)	$R_1 = 0.0338$, $wR_2 = 0.0902$	$R_1 = 0.032$, $wR_2 = 0.091$
R indices (all data)	$R_1 = 0.0487$, $wR_2 = 0.0952$	$R_1 = 0.038$, $wR_2 = 0.094$
$\Delta\rho_{max}/\Delta\rho_{min}$, e Å^{-3}	0.373/–0.283	0.33/–0.92

The unit cell parameters of the compound **II** were measured and found they were same as complexes **I**, so its crystallographic data weren't collected further. The complex **I** consist of the cation groups of formula $[Zn^{II}(H_2Biim)_2(H_2O)_2]^{2+}$ and terephthalate anions (Fig. 1a).

The metal(II) ion is six coordinate, having a distorted octahedron configuration with the axial sites being occupied by aqua ligands (Zn–O 2.229 Å). In complex, the H_2Biim ligands *trans*-coordinated (Zn–N(1) 2.113 Å and Zn–N(3) 2.145 Å). The NZnN bite angle generated by the chelating of the biimidazole in the complex is slight diversity (NZnN 80.40°). The angle is comparable to previously reported values [18–20].

The analysis of crystal structure of **I** reveals that it's interdigitated. Because of special geometry among COO^- group on terephthalic acid, uncoordinated amino of the biimidazole ligand and coordinated waters, extensive hydrogen bonds are formed. The cation $[Zn^{II}(H_2Biim)_2(H_2O)_2]^{2+}$ at both side of the divalention of terephthalate via charge assisted hydrogen bonds N–H···O (Fig. 2). The N···O distances are N(2)···O(1) 2.688, N(4)···O(2) 2.737 Å, respectively. In the anion, the carboxylate groups are rotated out of the plane of the aromatic ring, the mean tortional twist around C(7)–C(8) being 30.6° for **I**. So the supramolecular structure is dominated by the two principal hydrogen bonds between each coordinated H_2Biim ligand and carboxylate group (graph set $R_2^2(9)$) which served to link the ions into infinite cation···anion···cation chains. Ligand H_2Biim has only two N–H functionalities, both of which are tied up in the chain formation. In the absence of further N–H group, the linking of chains into sheets has to occur via another means. In the compound, it occurs via a hydrogen bond from an oxygen atom on the axial coordinated water molecule to the carboxylate oxygen atom O(2) (Fig. 2). An additional hydrogen bond between the carboxylate oxygen atom O(1) and the aqua oxygen atom of another sheet serves to link the sheets into a three-dimensional network (Fig. 3). Therefore, coordinating water molecules help to sustain the 2D-assembly and at the same time the final 3D-arrays.

Table 2. Selected bond distances (Å) and angles (deg) for complexes **I** and **III***

I			**III**		
Bond, *d*, Å	Measured	Calculated	Bond, *d*, Å	Measured	Calculated
Zn(1)–N(1)	2.1135(16)	2.0273	Cd(1)–O(1)	2.476(2)	2.2392
Zn(1)–N(3)	2.1452(15)	2.2348	Cd(1)–N(1)	2.323(2)	2.4727
Zn(1)–O(3)	2.2290(16)	2.3644	Cd(1)–N(2)	2.291(2)	2.4729
Angle, ω, deg	Measured	Calculated	Angle, ω, deg	Measured	Calculated
N(1)Zn(1)N(3)	80.41(6)	80.5074	O(1)Cd(1)N(1)	89.90(6)	84.7898
N(1)$^{\#1}$Zn(1)N(3)	99.59(6)	99.4912	O(1)Cd(1)N(1)$^{\#1}$	90.10(6)	95.2112
N(1)Zn(1)O(3)$^{\#1}$	90.11(7)	92.5009	O(1)Cd(1)N(2)	90.05(6)	95.2024
N(3)Zn(1)O(3)$^{\#1}$	88.60(6)	97.4794	O(1)Cd(1)N(2)$^{\#1}$	89.95(6)	84.7982
N(1)Zn(1)O(3)	89.89(7)	87.5018	N(1)Cd(1)N(2)	75.48(6)	70.6301
N(3)Zn(1)O(3)	91.40(6)	92.5179	N(1)Cd(1)N(2)$^{\#1}$	104.52(6)	109.374

* Symmetry transformations used to generate equivalent atoms for: $^{\#1}$ $-x, -y+1, -z+1$ (**I**); $^{\#1}$ $-x+1, -y+1, -z+1$ (**III**).

Table 3. Geometric parameters of hydrogen bonds for complexes **I** and **III***

Contact D–H···A	Distance, Å			Angle DHA, deg
	D–H	H···A	D···A	
		I		
N(2)–H(2*A*)···O(1)	0.860	1.846	2.688	165.75
N(4)–H(4)···O(2)	0.860	1.882	2.737	172.86
O(3)–H(3*B*)···O(l)$^{\#2}$	0.795	1.948	2.731	168.48
O(3)–H(3*A*)···O(2)$^{\#3}$	0.744	2.139	2.863	164.45
		III		
O(3)–H(3O)···O(4*A*)$^{\#2}$	0.82	1.82	2.628(2)	170
N(3)–H(3N)···O(1)$^{\#3}$	0.86	1.91	2.724(2)	158
N(4)–H(4N)···O(2)$^{\#3}$	0.86	1.84	2.701(2)	174

* Symmetry transformations used to generate equivalent atoms: $^{\#2}$ $-x+1, -y+1, -z+1$; $^{\#3}$ $x-1/2, -y+3/2, z-1/2$ (**I**); $^{\#2}$ $-x-1, -y+1, -z$; $^{\#3}$ $x-1, y, z$ (**III**).

With the present results, it is shown that the complexes **I** and **II** are isostructural (monoclinic, comparable cell dimensions, same space group, similar internal atomic coordinates). The complex **III**, however, does not contain any water molecules but the protonated terephthalate groups coordinated to the metal center. The molecular and crystal structures of **III** were illustrated in Figs. 1b, 4, 5. The structures are identical to those of $[Cd(H_2Biim)_2(HBDC)_2]$ [21] and detailed structure description is not presented here.

The IR spectra of complexes **I**–**III** exhibit a mediumintensity and broad band in the 3300–2540 cm^{-1} region which can be attributed to the N–H stretching vibration of H_2Biim and the O–H stretching vibrations of the H_2O molecules (**I** and **II**) or protonated terephthlate group (**III**). The strong and broad bands appeared in the 1567–1568 and 1397–1399 cm^{-1} regions in complexes **I** and **II** are ascribed to the asymmetric and symmetric stretching vibrations of the uncoordinated carboxylate groups of the terephthalate ligand, which are finally confirmed by an X-ray diffraction analysis. The IR spectrum of **III**, however, contains prominent $\nu(OCO_{as})$ and $\nu(OCO_s)$ stretching bands around 1588 and 1381 cm^{-1}, respectively. The relatively large value of ΔOCO ($\nu(OCO_{as}) - \nu(OCO_s)$) calculated for the complex (207 cm^{-1}) is close to the value expected for a unidentate coordination mode of the carboxylate moiety [22]. In the same time, the characteristic strong sharp bands at 1371 and 1692 cm^{-1} indicats the presence of C=O stretching vibration and protonated carboxylic group [10], respectively, which confirm the X-ray crystal structure.

The TGA result indicates that the complex **III** was stable up to about 300°C. The total weight loss of 84.02% between 300 and 900°C is consistent with the weight loss of H_2Biim and HTere ligands. The remain-

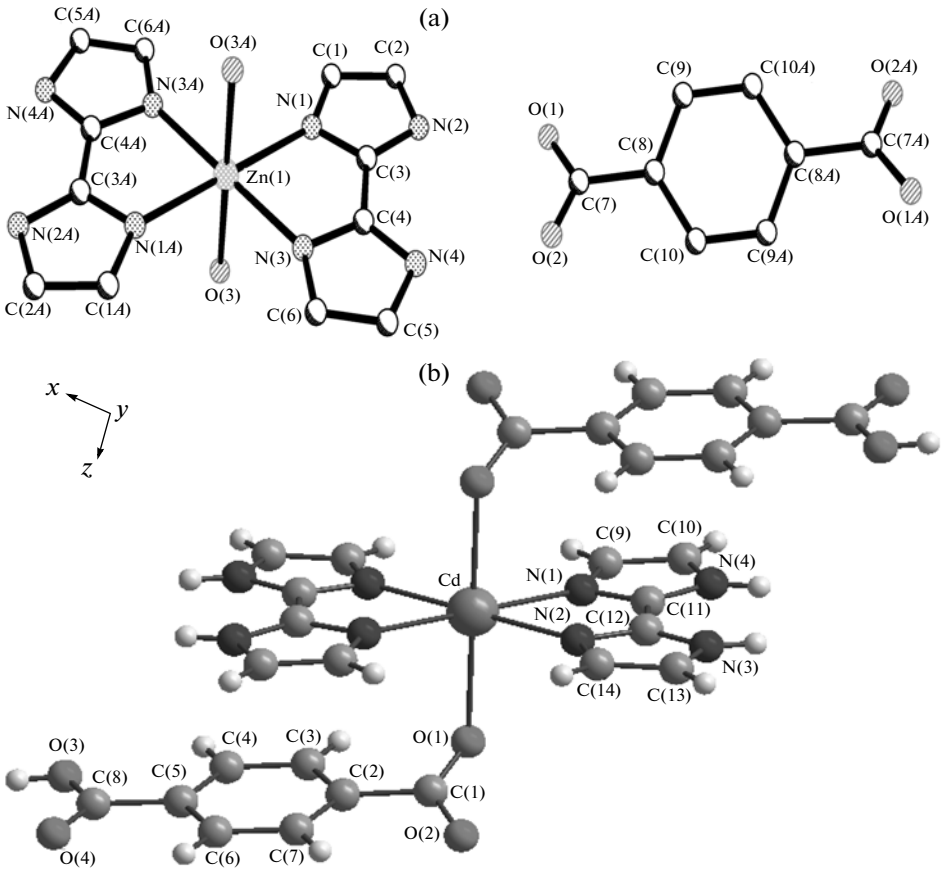

Fig. 1. The asymmetric unit of complexes **I** (a) and **III** (b).

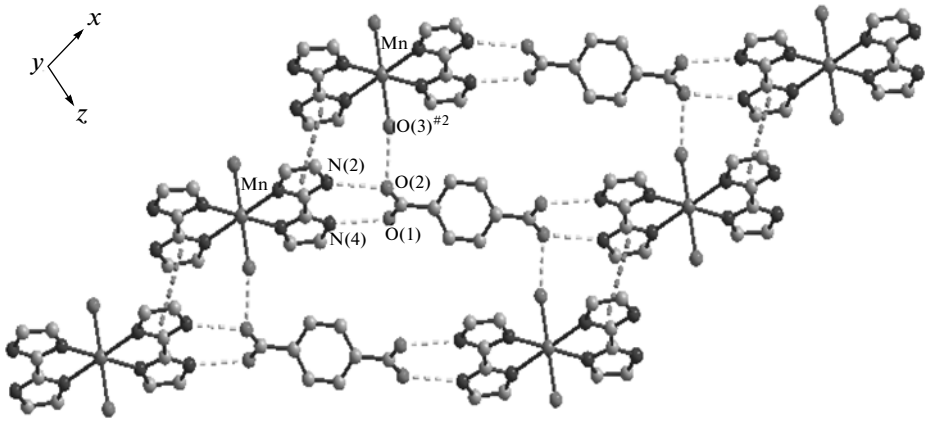

Fig. 2. Part of the hydrogen bonded sheets and π–π interaction present in the structure of complex **I** (H atoms are omitted for the sake of clarity).

ing weight of 17.04% is cadmium oxide that is in agreement with the calculated value of 18.03%. Thermal studies indicate that the anhydrous form of **III** exhibits higher thermal stability.

On the basis of the experimentation, theoretical calculations of the **I** and **III** complexes were carried out using the GAUSSIAN 03W program [23]. DFT with the B3LYP exchange-correlations is employed to optimize geometry structures, calculate vibration frequency and analyze electronic structures at the ground states throughout this work. Vibration frequency analyses are used to confirm the character of minima on the optimized structures. There is no symmetry constraints on these complexes studied in this work. For

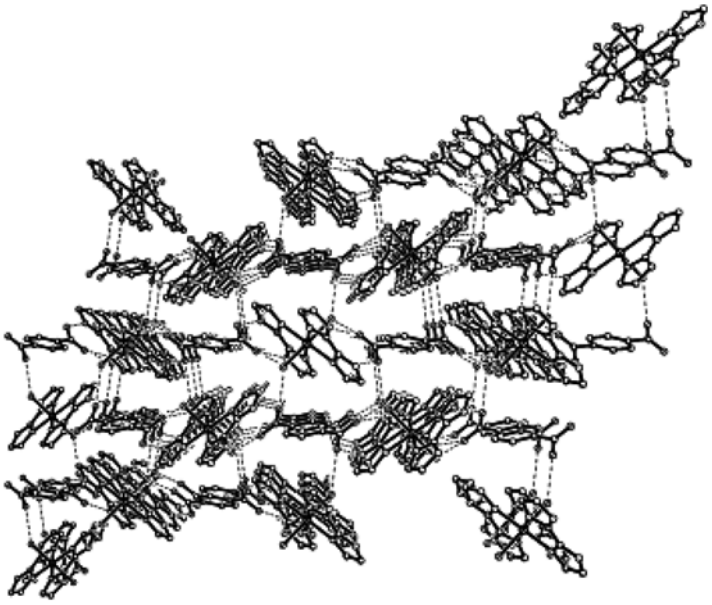

Fig. 3. Projection of 3D architecture of complex **I** (H atoms are omitted for the sake of clarity).

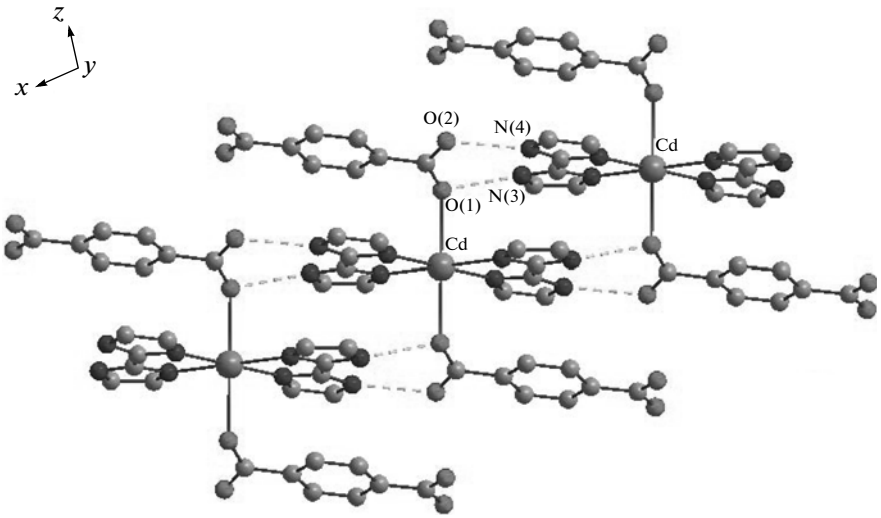

Fig. 4. Hydrogen bonds of complex **III** (H atoms are omitted for the sake of clarity).

ground state structural optimizations, the split valence plus polarization basis sets 6-31G(d) for nonmetal (H, C, N, S, O) atoms, and a double-ζ type LANL2DZ basis sets are used for metal atoms Pt. Calculated results show that metal Zn and Cd both exhibit six coordination modes, resulting into octahedral configurations of complex **I** and **III**. The main structural parameters of two complexes are summarized in Table 2 together with their partial X-ray crystal structures data. There are a little deviation between the calculation values and the experimental values. The main reason of the deviation is maybe as following: the approximation of calculation methods and setup basis sets, the neglecting anionic effect in the course of calculation, and the chemical environmental difference of the complexes (calculation was based on gas geometry configuration). And the deviation can be accepted in theoretical calculation for big system.

It is well known that frontier orbitals populations and energy gaps (ΔE_{L-H}) between HOMO and LUMO can reveal chemical bonding nature of molecules. The frontier orbitals populations of two complexes (**I** and **III**) are calculated and shown in Fig. 6. It is found that energy gap between HOMO and LUMO (ΔE_{L-H}) of **III** is the bigger than that of **I**. It revealed that complex **III** is more stable [24], and this results accorded with the experimental fact. From orbital populations

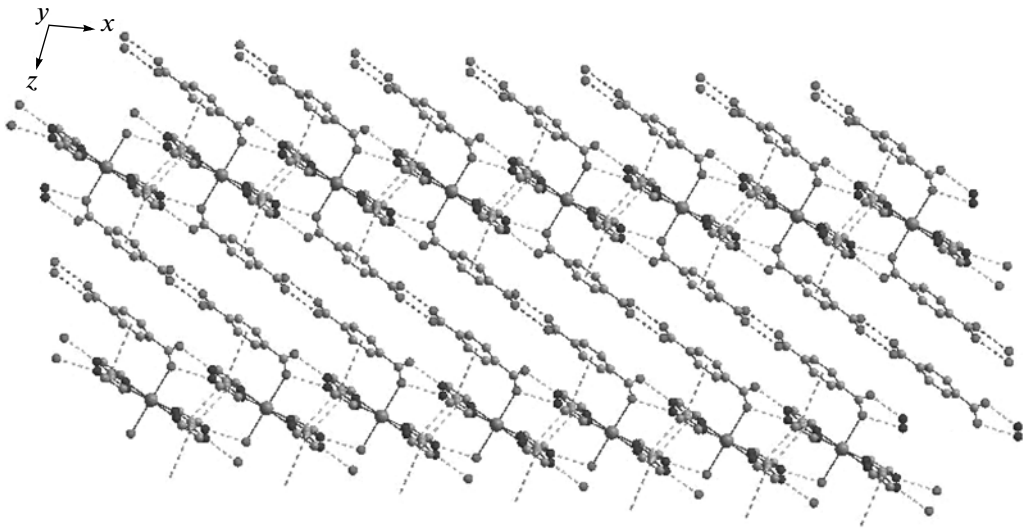

Fig. 5. The 2D sheet with quadrate latticework topology formed by hydrogen bonding and π–π interaction of complex **III** (H atoms are omitted for the sake of clarity).

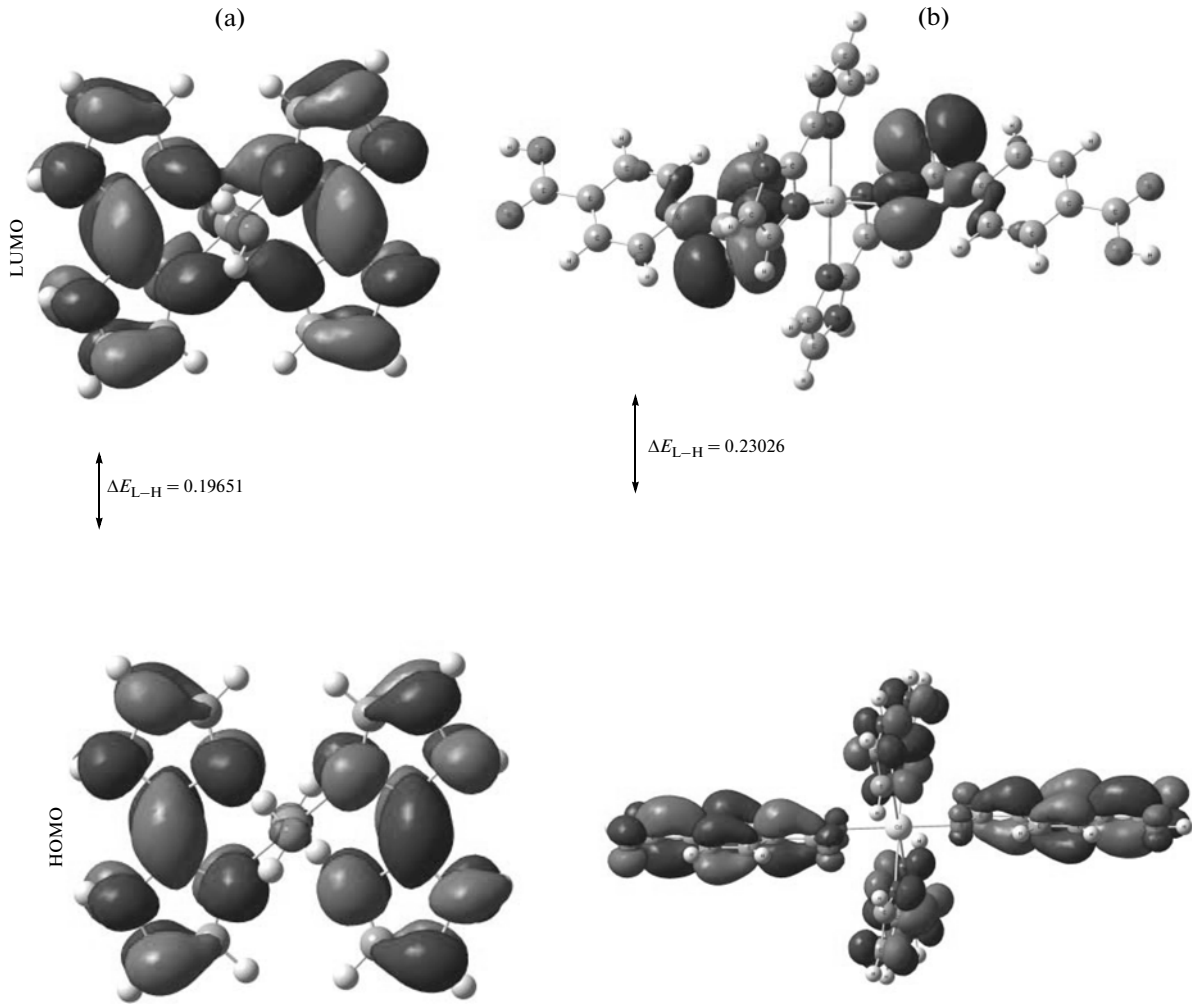

Fig. 6. Frontier orbitals topologies and energy gaps for complex **I** (a) and **III** (b).

Table 4. Milliken population analysis of complex **I** and **III**

Coordinated atoms	**I**	**III**
Zn/Cd	0.852730	1.057213
N(l)	–0.689337	–0.183865
N(2)	–0.68927	–0.183812
N(3)	–0.668635	–0.183863
N(4)	–0.66821	–0.183815
O(1)	–0.709125	–0.519678
O(2)	–0.709130	–0.519684

of two complexes, we also can see that metal Zn and Cd both have rare contributions to HOMO orbital of two complexes. It is inferred that the energies of metal *d* orbitals are bigger than that of π orbitals in organic ligands. From Milliken charge population analysis (Table 4), it can see that the positive charge of metal Cd is bigger than metal Zn, and negative charges of coordinated nonmetal atoms are smaller in complex **III** than in complex **I**. It is indicated that the metal Cd has stronger electron-donating ability than the metal Zn during the formational processing of complexes [25].

In additional, infrared spectra of complex **I** and **III** also have been calculated. Vibration frequency of two complexes are different. Typical C=C stretch frequency of both complexes are at 1700 cm^{-1}, and the intensity of C=C stretching vibration is the strongest in complex **I**. However, in complex **III**, the strongest vibration is C=O stretching at 1350 cm^{-1} and C=C stretching vibration is the second strong. Another obviously different vibration frequency lies near 1200 cm^{-1}, due to complex **III** has C–O stretching vibration, but complex **I** has not. Similarly, O–H bending vibration at 650 cm^{-1} can be found only in complex **III**. Thus the different compositions and structures between complex **I** and **III** can be obtained from infrared spectrum analysis.

ACKNOWLEDGMENTS

This work was supported by grants from the Educational Committee Foundation of Shaanxi Province (no. 2010JK884). We thank Prof. Seik Weng Ng for assistance with the X-ray diffraction studies.

REFERENCES

1. Ramirez, K., Reyes, J.A., Briceno, A., and Atencio, R., *CrystEngComm*, 2002, vol. 4, p. 208.
2. Carlucci, L., Ciani, G., Proserpio, D.M., et al., *Dalton Trans.*, 1997, p. 1801.
3. Su, C.Y., Cai, Y.P., Chen, C.L., et al., *J. Am. Chem. Soc.*, 2003, vol. 125, p. 8595.
4. Woodward, J.D., Backov, R.V., Abboud, K.A., et al., *Polyhedron*, 2006, vol. 25, p. 2605.
5. Wang, X.Y., Li, B.L., Zhu, X., et al., *Eur. J. Inorg. Chem.*, 2005, p. 3277.
6. Awaleh, M.O., Badia, A., Brisse, F., et al., *Inorg. Chem.*, 2006, vol. 45, p. 1560.
7. Pan, L., Huang, X.Y., Li, J., et al., *Angew. Chem.,* 2000, vol. 39, p. 527.
8. Pan, L., Huang, X.Y., and Li, J., *J. Solid State Chem.,* 2000, vol. 152, p. 236.
9. Hausmann, J.L., Jameson, G.B., and Brooker, S., *Chem. Commun.*, 2003, p. 2992.
10. Go, Y.B., Wang, X.Q., Anokhina, E.V., et al., *Inorg. Chem.*, 2005, vol. 44, no. 3, p. 8265.
11. Zheng, P.Q., Ren, Y.P., Long, L.Sh., et al., *Inorg. Chem.*, 2005, vol. 44, p. 1190.
12. Matsumoto, N., Motoda, Y., Matsuo, T., et al., *Inorg. Chem.*, 1999, vol. 38, p. 1165.
13. Qi, Zh.P., Bai, Zh.Sh., Yuan, Q., et al., *Polyhedron*, 2008, vol. 27, p. 2672.
14. Chermette, H., *Coord. Chem. Rev.,* 1998, vol. 178, p. 699.
15. Machura, B., Wolffl, M., Świtlickal, A., et al., *Struct. Chem.*, 2010, vol. 24, p. 761.
16. Fieselmann, B.F., Hendrickson, D.N., and Stucky, G.D., *Inorg. Chem.*, 1978, vol. 17, p. 2078.
17. Sheldrick, G.M., *SHELXL-97, Program for the Refinement of Crystal Structure*, Göttingen (Germany): Univ. of Göttingen, 1997.
18. Widlicka, D.W., Wong, E.H., Weisman, G.R., et al., *Inorg. Chem. Commun.*, 2000, vol. 3, p. 648.
19. Ye, B.H., Xue, F., Xue, G.Q., et al., *Polyhedron*, 1999, vol. 18, p. 1785.
20. Ghosh, A.K., Jana, A.D., Ghoshal, D., et al., *Cryst. Growth Des.,* 2006, vol. 3, p. 701.
21. Sang, R.L. and Xu, L., *Inorg. Chim. Acta*, 2006, vol. 359, p. 525.
22. Deacon, G.B. and Phillips, R.J., *Coord. Chem. Rev.*, 1980, vol. 33, p. 227.
23. Frisch, M.J., Trucks, G.W., Schlegel, H.B., et al., *Gaussian 03, Revision C.02,* Wallingford (CT, USA): Gaussian, Inc., 2004.
24. Ghiasi, R., *Russ. J. Coord. Chem.*, 2011, vol. 37, no. 1, p. 72.
25. Zhou, C.H., Zhu, H.Y., Wang, Y.Y., et al., *J. Mol. Chem.*, 2005, vol. 779, p. 66.